Astron. Astrophys. 347, 313–320 (1999)

ASTRONOMY AND ASTROPHYSICS

Low frequency plasma turbulence and high energy particles at CIR-related shock waves

H.-T. Claßen[1], **G. Mann**[1], **R.J. Forsyth**[2], **and E. Keppler**[3]

[1] Astrophysikalisches Institut Potsdam, An der Sternwarte 16, D-14482 Potsdam, Germany
[2] The Blackett Laboratory, Imperial College, Prince Consort Road, London, UK
[3] Max-Planck-Institut für Aeronomie, Postfach 20, D-37191 Katlenburg-Lindau, Germany

Received 1 February 1999 / Accepted 19 April 1999

Abstract. We present initial results from a survey of the low frequency magnetic field turbulence measured at the forward/reverse shock pairs associated with the interaction regions of high and low speed solar wind streams (CIRs). The magnetic field data are taken from vector helium and fluxgate magnetometer observations (VHM/FGM) aboard the Ulysses spacecraft between July 1992 and December 1993. A turbulence measure is defined as total wave power in the frequency range available from the raw data. This quantity is computed for the up- and downstream regions of the CIR-shocks and compared with the fluxes of 1 MeV protons and roughly 1 MeV/nucl. helium (Ulysses-EPAC measurements) at the time of shock crossing. We find a poor correlation between the upstream magnetic field turbulence and the high energy particle fluxes, and a high correlation between these quantities in the downstream region. The correlation between particle flux and field turbulence is best for the region roughly one gyroradius (of the high energy particles) downstream of the shock. Thus we conclude that wave-particle interactions in the downstream region, especially in the direct vicinity of the shock transition play an essential role for the acceleration of particles at CIR-related shock waves.

Key words: magnetic fields – plasmas – shock waves – turbulence – Sun: solar wind

1. Introduction

Wave-particle interactions play a fundamental role for our understanding of the physics of space plasmas, especially at collisionless shock waves. This becomes plain as soon as we notice that the plasma parameters at these structures change on a distance which is much smaller than the mean free path for Coulomb collisions. Thus the study of energy dissipation and particle acceleration at collisionless shocks requires a detailed analysis of non linear processes in low density plasmas at high temperatures. There are three different approaches to solve these problems.

1) An analytical treatment of coupled hydromagnetic wave excitation and ion acceleration at shocks – see e.g. Lee (1983) who solved coupled diffusion-transport and wave kinetic equations. 2) Computer simulations of particle acceleration at shocks – they can be divided into the test particle approach (e.g. Decker 1988), Monte Carlo simulations (e.g. Ellison et al. 1983), and hybrid simulations (e.g. Scholer et al. 1998). The main difference between these methods concerns the self-consistent coupling of accelerated particles and the up- and downstream waves. The Monte Carlo simulations contain free parameters, e.g., the scaling of mean free path with rigidity, which are computed self-consistently in the hybrid codes. Thus the Monte Carlo results can be fitted to the results of the hybrid codes (Ellison et al. 1993). 3) An observational survey of the different populations of energetic ions and their relation to low frequency magnetic field fluctuations – this was for instance done by Russell & Hoppe (1983) who reviewed the observations at the earth's bow shock.

The analysis presented in our paper is of the third type and can be specified as follows. The shocks under consideration here are neither travelling interplanetary shocks nor bow shocks but shock waves associated with corotating interaction regions (CIRs). These structures and the development of shocks at their boundaries are well-documented since the Pioneer 10 mission (Smith & Wolfe 1976; Gosling 1996). CIR-shocks develop from the interaction of high and low speed solar wind streams at large distances ($>$ 2–3 AU) from the sun: Their shock geometry is on average quasi-perpendicular (the angle θ_{Bn} between the shock normal and the upstream magnetic field lies between 45 and 90 degrees due to the inclination of the Parker spiral) and their Alfvén-Mach number $M_A = v_{sh}/V_A$ (the ratio of shock velocity and Alfvén speed) lies between 1.2 and 5. Furthermore it must be kept in mind that CIRs are connected with two different states of the solar wind phenomenon which partly show strong abundance anomalies (e.g. von Steiger 1995).

CIR-related shocks are a quasi-permanent source of highly energetic particles (cf. Fig. 2) – even in times of a quiet sun – and it is striking that in most cases the reverse shocks facing the fast solar wind are accompanied by a higher flux of energetic particles than the outward propagating forward shocks. Claßen et al. (1998) analysed the MHD-characteristics of 18 CIR-shock pairs and showed that the forward/reverse shocks are predominantly subcritical/supercritical in the sense of the first critical Alfvén-Mach number (e.g. Edmiston & Kennel 1984). Further-

Send offprint requests to: H.-T. Claßen (tclassen@aip.de)

more they showed that the highest fluxes of high energy protons and helium (1 MeV/nucl.) were observed for CIR-shocks with a sufficiently high Mach number ($M_A > 2.5$) and a θ_{Bn}-range between 50 and 70 degrees. Thus, there are hints for a different particle acceleration efficiency at CIR-related shocks and travelling interplanetary shocks which show the highest fluxes for $30^\circ \leq \theta_{Bn} \leq 60^\circ$ (van Nes et al. 1984).

Accordingly, the different angular ranges hint at different acceleration processes. Claßen et al. (1998) discussed the two well-known limiting cases of diffusive shock acceleration and argued that neither the pure forms of a first-order Fermi process nor shock-drift acceleration seem to be quite satisfactory. The first-order Fermi process (e.g. Kirk 1994, as review) is mostly considered at quasi-parallel shocks, i.e., $0^\circ \leq \theta_{Bn} \leq 45^\circ$, and the particles are essentially accelerated during multiple scattering between low frequency plasma waves in the up- and downstream region. In the pure form of shock-drift acceleration (e.g. Armstrong et al. 1985) particles are accelerated during a single shock encounter with the shock transition zone. The particles drift immediately inside the shock front and then leave the shock (there is no multiple scattering); the velocity gain of the particles is $\propto v_{sh} \sec \theta_{Bn}$ and thus increases rapidly with increasing θ_{Bn}.

The paper in hand focusses on an analysis of the correlation between the wave activity in the up- and downstream region of these shocks and the number of accelerated particles. In order to establish such a study we correlate two single quantities – the total wave power as a turbulence measure and the particle flux at the time of shock crossing as a measure for the acceleration efficiency. The method of our data analysis is described in the next section. The aim of these investigations is twofold. First we want to localize the regions of intensive wave-particle interaction and secondly we want to find possible acceleration mechanisms at CIR-related shocks. From the second point of view we do not take the diffusion approximation for granted. This will be discussed in Sect. 3 but it should be clear that our study is in an initial stage.

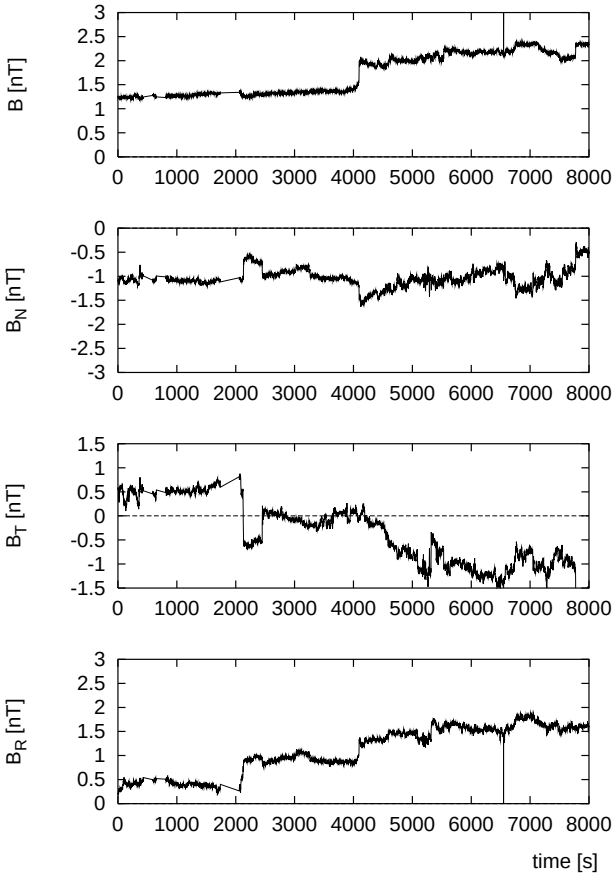

Fig. 1. Magnetic field components and magnitude in solar-polar coordinates (RTN) with a time resolution of 2 s for forward shock of CIR # 5 (Ulysses VHM/FGM measurement). The shock occurs on 08 Oct., 1992, 06:16:00 UT corresponding to second 4096 on the time axis.

2. Data analysis

The data analysed in this section complete the investigations of Claßen et al. (1998) concerning the Ulysses CIR-encounters between July 1992 and 1993. The new results are due to the high time resolution magnetic field data from the VHM/FGM-experiment aboard Ulysses. Detailed information about these magnetometers can be found in Balogh et al. (1992). Although the highest time resolution of the instruments is 1 s, we consequently took 2 s-averaged magnetic field data in order to analyse all CIR-encounters with the same precision. Fig. 1 shows an example of the magnetic field measurements during the Ulysses encounter with the reverse shock on 08 Oct., 1992, 06:16:00 UT. In the following text we will use the numbering from Bame et al. (1993) and this shock will be refered to as CIR # 5. We chose this example to show the different behaviour of the single magnetic field components which can exhibit torsional waves or rotational discontinuities. A survey of the proton and helium fluxes at the shocks under consideration in this paper is shown in Fig. 2. The peaks labelled with numbers are related to CIRs and we took a closer inspection of the CIRs 1–18 since these shocks were accompanied by the largest number of high energy particles.

In order to quantify the magnetic field turbulence in the up- and downstream region of the shocks we applied the standard method for spectral analysis – a fast Fourier transformation (e.g. Yuen & Frazer 1979). According to this theory there are two frequency limits for such an analysis. First, the Nyquist frequency $f_{\max} = f_{\mathrm{Ny}} = 1/2t_{\min} = 0.25\,\mathrm{Hz}$ as an upper limit given by the sampling frequency of 2 s, and secondly, the inverse of the total sampling time $f_{\min} = 1/t_{\max}$ as a lower limit. An example of the spectrum of the upstream turbulence of shock # 5F is shown in Fig. 3. For this figure we used a standard FFT-procedure for the magnitude and the RTN-components (solar polar coordinates) of the magnetic field for a total sampling time of 4096 s, i.e., roughly 1 hour. Thus the two frequency limits are given by $2.4 \cdot 10^{-4}$ and 0.25 Hz. Concerning the different behaviour of magnitude and single components of the magnetic field it can be seen that the differences lead to different slopes and absolute values of the Fourier coefficient but they show no clearly distinct peaks. For the further analysis, i.e., a comparison

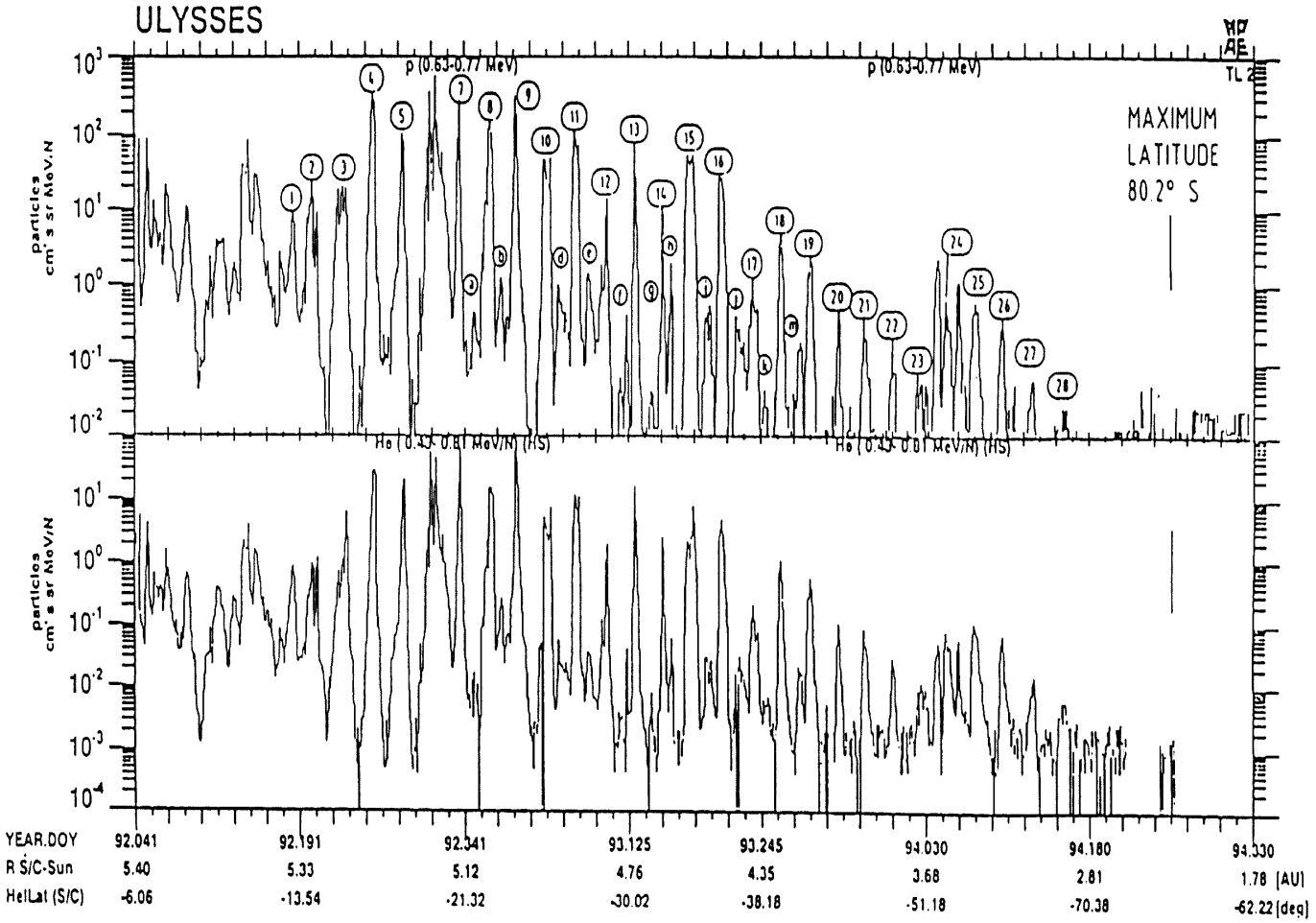

Fig. 2. Variation of the particle flux (protons and helium) during Ulysses' journey to the south pole. The numbers label CIR-related shocks and the letters travelling interplanetary shocks or solar particle events.

of the total wave power in this frequency range, it is necessary to substract the mean value of the magnetic field before the spectral analysis. This is essential since a constant magnetic field does not lead to a perfect Dirac peak but to a triangle shaped spectrum with a width depending on sampling rate and time and thus changes the results for the total wave power. Thus, since we are interested just in the fluctuating part of the spectrum, we define the total sum of the magnitude of the Fourier coefficients $F(i)$ taken from a magnetic field with a zero average within those frequency limits as turbulence measure, i.e.,

$$T_{\mathrm{up/down}} = \sum_{i=f_{\min}}^{f_{\max}} |F_{\mathrm{up/down}}(i)| \,. \tag{1}$$

Here it should be mentioned that the Fourier coefficients are equidistant in frequency-space. The indices 'up' and 'down' refer to the Fourier analysis in the upstream and downstream region, respectively. Shocks with data gaps were treated in the following way. If the gaps were not too big, i.e., smaller than 5% of the total sampling time we took a linear interpolation from the first to the last data point around the gap (cf. Fig. 1). Shocks with bigger data gaps were not analysed. Thus we investigated a number of 26 (31) CIR-related shocks with a total sampling time of 4096 (512) s from the total number of 32 in Claßen et al. (1998).

The next step in our analysis is the correlation between the total flux of 1 MeV protons as evaluated in that paper and the turbulence measure defined in Eq. (1). This is displayed in Fig. 4 which shows the logarithm of 1 MeV proton flux averaged over 60 minutes at the time of shock crossing plotted against the turbulence measure $T_{\mathrm{up/down}}$ determined for magnitude of the magnetic field. With reference to Claßen et al. (1998) two things should be mentioned. First, that the 1-hour averages are required by the statistics, i.e., we need enough high energy particles exciting the detectors. Secondly, that it would be better to take the particle flux up- and downstream of the shock transition. According to this fact it should be noticed that that the maximum deviation between the up-/downstream flux and the flux at the time of shock crossing comes to a factor of 3, i.e., the biggest possible error bars in Fig. 4 concerning $\log j_p$ are 0.5. The dotted lines in this figure show the best linear fit, r and p are the correlation coefficient and the probality for a lucky coincidence. As a first result one should realise that there is a good correlation ($r = 0.51$) between the downstream turbulence and the proton flux and a weak correlation ($r = 0.23$) between upstream

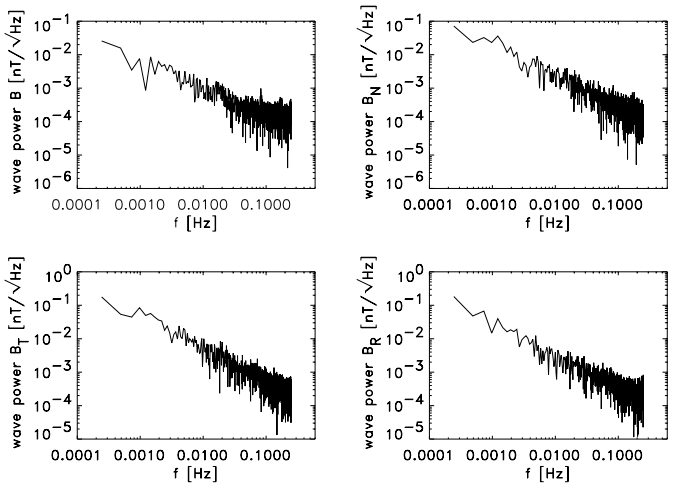

Fig. 3. Spectral analysis of shock # 5F (upstream region) for the magnitude and the RTN-components of the magnetic field on a double-logarithmic scale. The sampling rate is 2 s and the total sampling time 4096 s.

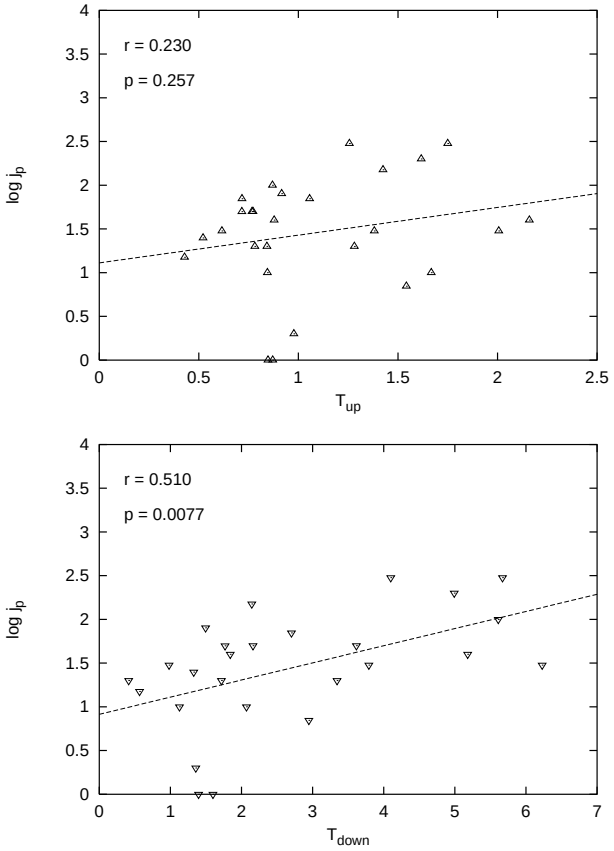

Fig. 4. Correlation between the flux of 1 MeV protons at the time of shock crossing and the turbulence measure defined in Eq. (1). The proton flux is 1-hour averaged and the turbulence measure is determined for the magnitude of the magnetic field and a total time of 4096 s. r is the correlation coefficient of the linear fit indicated by the dotted line, p the probability to achieve such a distribution by chance.

turbulence and proton flux. The correlation coefficients for the single components show a slightly weaker correlation. We obtain $r_{R,T,N} = 0.41,\ 0.42,\ 0.46$ for the downstream correlation and $r_{R,T,N} = 0.19,\ 0.12,\ 0.07$ for the upstream correlation.

The results of the turbulence analysis in the direct vicinity of the shock transition region is shown in Fig. 5. Here, it seems to be useful to choose a distance roughly one gyroradius upstream and downstream of the shock, respectively. Thus, with $\rho_{cp}\,(\mathrm{km}) \leq 4,600 \cdot W^{1/2}(\mathrm{keV})/B(\mathrm{nT})$ and W as kinetic energy, we can estimate a proton gyroradius of roughly 200,000 km for 1 MeV protons in the vicinity of our CIR-related shocks. This distance corresponds to a time of 400 s for an average solar wind speed of 500 km s^{-1} and we took of FFT-algorithm with $256\ \mathrm{points} = 512\,\mathrm{s}$. The results from Fig. 5 strengthen the trend from Fig. 4. Now there is less evidence for a correlation between the proton flux and magnetic field turbulence in the upstream region ($r = 0.01$) and very high evidence for a correlation of these quantities in the downstream region ($r = 0.66$). On the other hand we found that the correlation with the magnetic field components is only slightly changed, i.e., $r_{R,T,N} = 0.41,\ 0.45,\ 0.45$ immediately downstream and $r_{R,T,N} = 0.12,\ 0.09,\ 0.01$ immediately upstream, respectively.

The previous results were related to roughly 770–990 keV protons but they were confirmed by the analysis of 700–800 keV/nucl. helium particles measured by the EPAC-instrument aboard Ulysses. Since the plots look quite similar we just write down the changes in the analysis of the correlation between helium flux and the low frequency wave turbulence. In order to get high enough counting rates we took 2 hour averages for the determination of the helium flux and correlated it with the turbulence measure (with respect to the magnetic field magnitude) determined for the same duration. Thus we obtained correlation coefficients of $r = 0.25$ and $r = 0.46$ for the upstream and downstream region, respectively. Furthermore, we found the same trend as already described for the protons when we moved closer to the shock vicinity. Taking into consideration that the gyroradius of the analysed helium should be roughly 4 times larger than the protons from Fig. 5 we choose a FFT algorithm of 1024 points. This analysis results in correlation coefficients of $r = 0.03$ and $r = 0.53$ for the regions immediately upstream and downstream of the shock.

3. Discussion

In the previous section we introduced a turbulence measure at CIR-shocks and related this quantity from Eq. (1) to the proton and helium flux in order to determine the acceleration process at these shocks. The analysis of Claßen et al. (1998) showed that shock waves with a high magnetic field jump and a quasi-perpendicular geometry ($50^\circ \leq \theta_{Bn} \leq 75^\circ$) are those with the highest particle flux. Furthermore, it seemed very likely that the most efficient particle accelerating shocks are supercritical in the sense of the first critical Mach number (e.g. Edmiston & Kennel 1984).

This Mach number tells us something about the dissipation and turbulence at shock waves: Subcritical shocks are laminar shocks with a steplike magnetic field behaviour and little

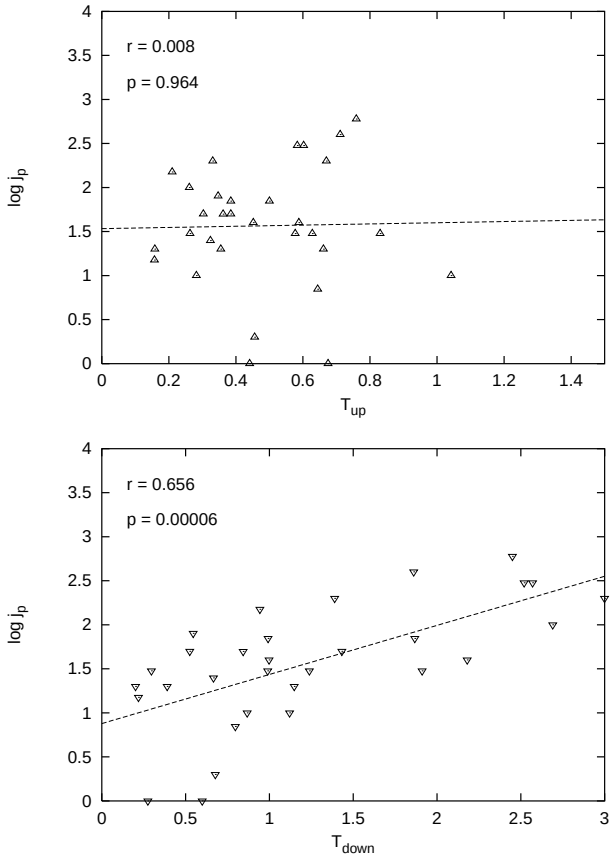

Fig. 5. Correlation between the flux of 1 MeV protons (1-hour averaged) at the time of shock crossing and the turbulence measure (Eq. (1)) for the magnitude of the magnetic field and a total sampling time of 512 s.

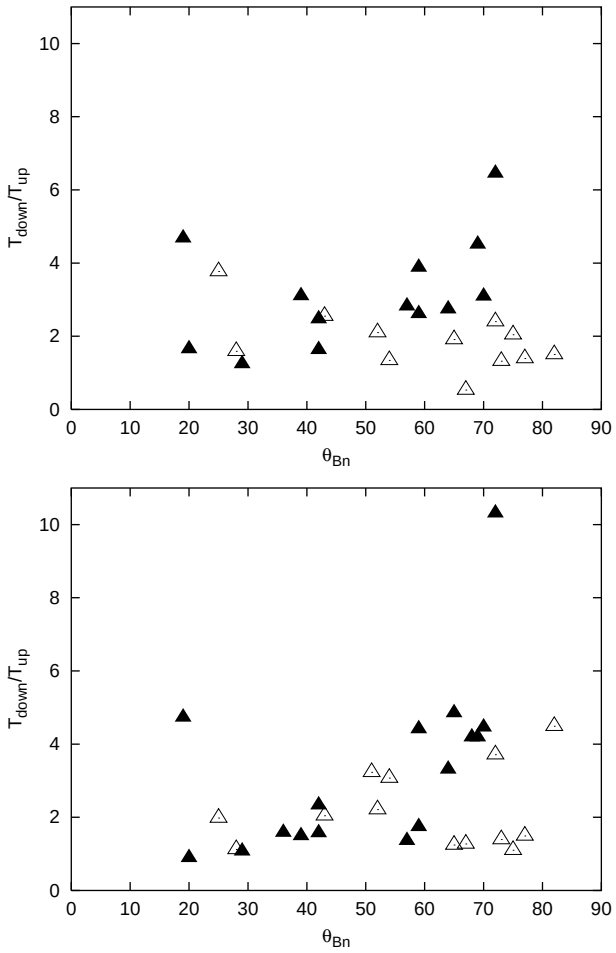

Fig. 6. $T_{\rm down}/T_{\rm up}$ versus shock geometry, θ_{Bn}, for a total sampling time of 4096 s (*upper panel*) and 512 s (*lower panel*), respectively. The open/filled triangles indicate sub-/supercritical shock waves according to an analysis based on MHD-characteristics (Claßen et al. 1998).

turbulence (e.g. Mellot 1985). Supercritical shocks are accompanied by a higher degree of turbulence and are structured on different length scales (e.g. Kennel et al. 1985). Especially, they show a high turbulence in both up- and downstream region for quasi-parallel shocks and low/high turbulence in the upstream/downstream region of quasi-perpendicular shocks (e.g. Greenstadt 1985). Thus the shock from Fig. 1 is a slightly supercritical, quasi-perpendicular shock wave.

A natural distinction between quasi-parallel ($\theta_{Bn} < 45°$) and quasi-perpendicular shocks ($\theta_{Bn} > 45°$) is based on the analysis of the guiding center motion of ions specularly reflected off the shock transition (Schwartz et al. 1983). As these authors show, the guiding center velocity is directed upstream and downstream for quasi-parallel and quasi-perpendicular shocks, respectively. This means that the reflected ions at quasi-parallel shocks can possibly contribute to the wave generation in the upstream region while such a process is not possible for quasi-perpendicular shocks.

Fig. 6 is a quantitative test for the quality of the turbulence measure (Eq. 1) in relation to the MHD analysis in Claßen et al. (1998). The figure shows how the ratio of the turbulence measures in the down- and upstream regions depend on θ_{Bn} for a averaging time of 4096 (upper panel) and 512 s (lower panel), respectively. It was calculated for the magnitude of the magnetic field but the single components show quite similar results. The filled and open triangles are supercritical and subcritcal shocks according to the MHD analysis using long time averaged data. While the lower panel shows only rough trends the upper panel with a total sampling time of 4096 s agrees with the previous annotations. Although the statistics is not to high, we can see that the ratio $T_{\rm down}/T_{\rm up}$ for supercritical, quasi-perpendicular shocks is significantly greater than for the subcritcal shocks. For the quasi-parallel shocks there seems to be no clear differences – a fact which was also expected from the previous explanations. Thus we can conclude that the ratio $T_{\rm down}/T_{\rm up}$ for a sampling time of roughly 1 hour can be regarded as a good measure for an analysis of the critical behaviour of quasi-perpendicular shocks while a total sampling time of 512 s – at least in the vicinity of the shock transition – seems to be too short. On the other hand, if we compare the results from Figs. 4 and 5, we find much clearer results for the correlation between 1 MeV proton flux and turbulence in the direct vicinity of the shock transition. This seems to be crucial in the context of possible acceleration mechanisms.

In most cases the energy gain of charged particles at shock waves is studied via transport equations in the diffusion approximation (e.g. Axford et al. 1977) or scatter free shock-drift acceleration (e.g. Armstrong et al. 1985). On the other hand it was shown by Jokipii (1982, 1987) that diffusive acceleration also contains drift effects. From this point of view shock waves related to CIRs are ideal candidates for the theory developped in these papers. But it must be kept in mind that scattering might be insufficient and that the diffusion approximation is not practicable. Thus the following discussion focusses on the individual processes which are assembled in the transport equation.

Diffusion approximation (first-order Fermi process): The particles gain energy due to multiple reflections at magnetic irregularities in the upstream and downstream region and relax to a nearly isotropic angular distribution. Furthermore we should basically expect power law spectra with a spectral index only dependend on the compression ratio of the shock for the steady-state solution.

These predictions were partly checked in Claßen et al. (1998) and the tests are continued in our present paper. Thus, we found a rather *anisotropic* particle distribution in the shock vicinity (as expected by shock-drift effects) and power law indices nearly *independent* of the density compression ratio (see Fig. 4 in Claßen et al. 1998). There might be a couple of reasons for these results: First they could mean a restriction of the validity of the diffusion approximation. Such a possibility was taken in consideration by Jokipii (1987). Secondly – if we try to describe our results with the predictions of diffusion theory – there is also a variety of solutions. First, a non steady-state behaviour which could imply a correlation between the flux of accelerated particles and the turbulence in both the upstream and the downstream region. This is not in agreement with our present analysis. Secondly, we have to keep in mind that the power law is only a first approximation which is influenced by adiabatic deceleration (Fisk & Lee 1980) and by the spectrum of the injected particles (e.g. Blandford & Ostricker 1978).

At the present stage of our analysis it is difficult to say which of all these possibilities decide the issue but in our eyes two things should be analysed in greater detail. First the strong correlation between particle flux and wave turbulence in rather localized regions downstream of the shocks and secondly the poor correlation upstream. The first result leads to a discussion of locally acting acceleration mechanisms and the second results leads to a search for possible upstream scatter centers to justify the diffusion approximation.

Transit-time damping: Transit-time damping is the magnetic analogue to Landau damping and leads to an energy conversion from magnetic energy (of waves) to kinetic energy (of particles). Thus, this mechanism is a locally acting acceleration of particles via wave-particle interactions - especially between particles and fluctuations in the magnitude of the interplanetary magnetic field (e.g. magnetosonic waves). Now the results from the previous section suggest that the correlation between particle flux and turbulence measure is higher for a turbulence which is connected with changes in the *magnitude* of the magnetic field. Since transit-time damping is based on such kind of gradients of the magnetic field (Stix 1992) it cannot be ruled out that this mechanism contributes to the generation of high energy particles as suggested e.g. by Fisk (1976). On the other hand it should be clear that the differences in correlation for compressional and non-compressional wave turbulence are not very large and the best correlation is found only for a small region directly downstream of the shock transition. Nevertheless one should analyse these regions with respect to wave modes suitable for transit-time damping.

Shock-drift effects: The particles gain energy in a single reflection in the transition region of the shock leading to field aligned anisotropies in the particle distribution. This seems to be in agreement with our data analysis and could in particular explain the results from Fig. 5, i.e., the very good correlation between downstream turbulence and 1 MeV particle flux. Furthermore, the data analysis from our previous paper showed that a high magnetic field compression is a very good indicator for a high particle flux. Here, it should be mentioned that the magnetic field compression $r_B = |B_{\rm down}|/|B_{\rm up}|$ controls the number of reflected particles. Thus, if we assume for instance the conservation of the first adiabatic invariant (e.g. Leroy & Mangeney 1984), we obtain a critical loss cone angle $\alpha_{lc} = \arcsin(1/\sqrt{r}_B)$ showing that the number of reflected and accelerated particles increases with an increasing magnetic field compression. On the other hand it should be clear that this description might be too simple. Thus we find from the high resolution magnetic field data that the magnetic field changes not smoothly over the particle's gyroradius as required by adiabatic theory.

Furthermore, it seems again to be necessary to look for upstream scatter centers which would enable multiple shock encounters. This is a consequence from the fact that a single shock encounter does not produce enough highly energetic particles – at least not from a Maxwellian background. A scenario of this type was developped in the computer simulation of Decker & Vlahos (1986) who included transverse MHD-waves in the upstream region of quasi-perpendicular shocks. Although it should be clear that these test particle calculations do not tell the whole story (they are neither self-consistent nor do they enable cross field diffusion) they show that specific wave modes and not a total wave power would add multiple scattering to the shock-drift mechanism. Thus the efficiency of this process would be raised to a higher power. An similar scenario leading to multiple shock encounters in connection with shock-drift acceleration was discussed by Erdös and Balogh (1994). In their mechanism the backscattering to the shock transition is enabled by a special magnetic field topology where the field lines are curved back to the shock. From this point of view there is no need for upstream scatter centers in form of waves and the weak correlation between the upstream wave turbulence and the particle flux would not be surprising.

Finally, we must focus our attention on the finite range of our data. This means especially the finite frequency range in Fig. 3 and the fact that we only look at roughly 1 MeV/nucl. particles. Therfore we have to relate the frequency range of our data set to the cyclotron frequency as a typical frequency for low frequency

plasma waves (e.g. Krall & Trivelpiece 1986). This frequency is determined by the magnetic field strength and can be computed via $\omega_c = qB/m$, with the particle's charge q and mass m as constants. Taking an overall average of the magnetic field strength observed at the CIR-related shocks under consideration we obtain a field strength of 0.9 nT and thus a proton cyclotron frequency $\omega_{cp} = 0.085\,\mathrm{s}^{-1}$. The situation for the analysed helium particles is ambiguous since the EPAC-instrument cannot determine the charge of the particles (Keppler et al. 1992). In principle, there are two possibilities: either $\omega_{cHe} = \omega_{cp}/2$ or $\omega_{cHe} = \omega_{cp}/4$.

Furthermore, we must keep in mind the Doppler shift between the spacecraft frame (index sc) and the solar wind frame (index o) given by (e.g. Tsurutani et al. 1983)

$$\omega_{sc} = \omega_o \left(1 + \frac{v_{sw}}{v_{ph}} \cos\theta\right) , \qquad (2)$$

with v_{sw} and v_{ph} as solar wind velocity and phase velocity of the wave which propagates at an angle θ to the solar wind. Taking $v_{sw} = 500\,\mathrm{km\,s}^{-1}$, $v_p = V_A = 40\,\mathrm{km\,s}^{-1}$ (Alfvén velocity), and $\theta = 75°$ (Parker spiral) as rough estimations we obtain a proton cyclotron frequency of $f_{cp,sc} = \omega_{cp,sc}/2\pi = 0.06\,\mathrm{Hz}$ in the spacecraft frame. For helium the corresponding cyclotron frequency is either $f_{cHe,sc} = 0.03\,\mathrm{Hz}$ or $f_{cHe,sc} = 0.015\,\mathrm{Hz}$. Comparing this value with the panels from Fig. 3 it can be seen that the high frequency limit of the waves under consideration is well covered by our data. The low frequency limit of our analysis is given by the total sampling time and results in $f_{\mathrm{low}} = 0.002\,\mathrm{Hz}$ for the 512 s data and $f_{\mathrm{low}} = 0.00024\,\mathrm{Hz}$ for the 4096 s data. Thus the different correlation coefficients in Figs. 4 and 5 for the upstream region might indicate that the wave-particle interaction takes place in the lower part of the wave spectrum – at least for the particles we are looking at.

4. Summary

In our paper we analysed the correlation between the low frequency plasma waves and energetic particles (1 MeV/nucl.) with the aim to find out possible acceleration processes at CIR-related shocks.

The used approach did not analyse specific wave modes but introduced a turbulence measure in form of a total wave power in a given frequency range (see Eq. 1). This was established via a standard FFT-algorithm. With the help of this quantity we could reproduce the results from our previous study based on MHD-methods to determine the critical Mach number of the CIR-related shocks (see Fig. 6). Thus this result confirmed the quality of the introduced turbulence measure. Furthermore, the following results were obtained.

The high energy proton and helium flux is strongly correlated to the turbulence in the downstream region while the correlation to the upstream waves is rather poor (see Fig. 5). Especially, the region immediately downstream of the shocks indicates the existence of strong wave-particle interactions in the analysed data range.

Although one should be careful with final statements about the acceleration process of the analysed particles our results strongly favour a locally acting acceleration mechanism in the vicinity of the shock transition, e.g., a non-adiabatic shock drift acceleration or transit-time damping. Some uncertainties result from the finite range of our data analysis. Furthermore, a detailed wave analysis seems to be necessary. Such a analysis, e.g., the search for magnetosonic waves, is for instance required if we want to check the influence of transit-time damping. On the other hand, if we discuss a shock-drift effects, it seems to be necessary to enable multiple shock encounters. This could for instance be achieved by a specific field line configuration in the further shock vicinity.

Acknowledgements. The research of H.-T. C. was supported by DLR (DARA) under grant no. 50 ON 9601 0.

References

Armstrong T.P., Pesses M.E., Decker R.B., 1985, In: Tsurutani B.T., Stone R.G. (eds.) Collisionless Shocks in the Heliosphere: Reviews of Current Research. AGU GN-35, Washington D.C., p. 271
Axford W.I., Leer E., Skadron G., 1977, Proc. 15th Int. Cosmic Ray Conf. 11, 132
Balogh A., Beek T.J., Forsyth R.J., et al., 1992, A&AS 92, 221
Bame S.J., Goldstein B.E., Gosling J.T., et al., 1993, Geophys. Res. Lett. 20, 2323
Blandford R.D., Ostricker J.P., 1978, ApJ 221, L29
Claßen H.-T., Mann G., Keppler E., 1998, A&A 335, 1101
Decker R.B., 1988, Space Sci. Rev. 48, 193
Decker R.B., Vlahos L., 1986, J. Geophys. Res. 91, 13, 349
Edmiston J.P., Kennel C.F., 1984, J. Plasma Phys. 32, 411
Ellison D.C., Giacolone J., Burgess D., Schwartz S.J., 1993, J. Geophys. Res. 98, 21085
Ellison D.C., Jones F.C., Eichler D., 1983, J. Geophys. 50, 110
Erdös G., Balogh A., 1994, ApJS 90, 553
Fisk L.A., 1976, J. Geophys. Res. 81, 4633
Fisk L.A., Lee M.A., 1980, ApJ 237, 620
Gosling J.T., 1996, ARA&A 34, 35
Greenstadt E.W., 1985, In: Tsurutani B.T., Stone R.G. (eds.) Collisionless Shocks in the Heliosphere: Reviews of Current Research. AGU GN-35, Washington D.C., p. 169
Jokipii R.J., 1982, ApJ 255, 716
Jokipii R.J., 1987, ApJ 313, 842
Kennel C.F., Edmiston J.P., Hada T., 1985, In: Stone R.G., Tsurutani B.T. (eds.) Collisionless Shocks in the Heliosphere: A Tutorial Review. AGU GN-34, Washington D.C., p. 1
Keppler E., Blake J.B., Hovestadt D., et al., 1992, A&AS, 92, 317
Kirk J.G., 1994, In: Benz A.O., Courvoisier T.J.-L. (eds.) Plasma Astrophysics. Saas-Fee Advanced Course 24, Springer-Verlag, Berlin, Heidelberg, p. 224
Krall N.A., Trivelpiece A.W., 1986, Principles of Plasma Physics. McGraw-Hill, New York
Lee M.A., 1983, J. Geophys. Res. 88, 6109
Leroy M.M., Mangeney A., 1984, Ann. Geophys. 2, 4, 449
Mellot M.M., 1985, In: Tsurutani B.T., Stone R.G. (eds.) Collisionless Shocks in the Heliosphere: Reviews of Current Research. AGU GN-35, Washington D.C., p. 131
Russell C.T., Hoppe M.M., 1983, Space Sci. Rev. 34, 155
Scholer M., Kucharek H., Trattner K.J., 1998, Adv. Sp. Res. 21, 533

Smith E.J., Wolfe J.H., 1976, Geophys. Res. Lett. 3, 137
Schwartz S.J., Thomsen M.F., Gosling J.T., 1983, J. Geophys. Res. 88, 2039
von Steiger R., 1995, AIP Conference Proceedings 382, 193
Stix T.H., 1992, Waves in Plasmas. American Institut of Physics, NY
Tsurutani B.T., Smith E.J., Jones D.E., 1983, J. Geophys. Res. 88, 5645
van Nes P., Reinhard R., Sanderson T.R., Wenzel K.P., Zwickl R.D., 1984, J. Geophys. Res. 89, 2122
Yuen C.K., Frazer D., 1979, Digital spectral analysis. Csiro, Melbourne